Available online at www.sciencedirect.com
ScienceDirect
Catalysis Today 126 (2007) 44–53
CATALYSIS TODAY
www.elsevier.com/locate/cattod

Fluorescence microscopy: Bridging the phase gap in catalysis

Maarten B.J. Roeffaers [a], Johan Hofkens [b], Gert De Cremer [a], Frans C. De Schryver [b], Pierre A. Jacobs [a], Dirk E. De Vos [a], Bert F. Sels [a,*]

[a] *Centre for Surface Chemistry and Catalysis, Katholieke Universiteit Leuven, Kasteelpark Arenberg 23, 3001 Heverlee, Belgium*
[b] *Department of Chemistry, Katholieke Universiteit Leuven, Celestijnenlaan 200F, 3001 Heverlee, Belgium*

Available online 30 April 2007

Abstract

While many *operando* techniques focus on gas phase reactions, there is a growing need to look at working catalysts in the liquid phase. Fluorescence microscopy is a promising technique for bridging this phase gap. Like cellular biology, catalytic science may take advantage from the high spatiotemporal resolution and sensitivity of fluorescence microscopy. Earlier applications of fluorescence techniques in the study of diffusion or chemical transformation on inorganic solids are reviewed. The potential of fluorescence microscopy in catalysis is illustrated by data on acid-catalyzed transformation of fluorogenic organics on a mordenite zeolite.

Keywords: Fluorescence microscopy; Phase gap; Zeolite; Single molecule; Layered double hydroxides

1. Introduction

In the early days of catalytic science, catalysts were treated as black boxes. Improvements of catalytic performance were largely based on trial-and-error. In a later, more scientifically founded approach, detailed kinetic studies were combined with physicochemical catalyst characterization. However, as these physical studies were typically performed *ex situ*, or using deactivated, '*post mortem*' catalysts, it remained difficult in many cases to unambiguously relate molecular surface structure to catalytic performance. A more rational and efficient catalyst design is strongly dependent on insights in the molecular processes at the catalyst particle. This has been the major incentive for introducing *in situ* spectroscopic techniques in catalytic research.

Instrumental and technological advances in the previous decade made it possible to study the molecular events that take place at a heterogeneous catalyst under reaction conditions. Initially use was made of techniques and instruments with a low sensitivity, and with limited spatial or temporal resolution, *e.g.* based on IR, Raman or UV–vis spectroscopy. Despite their merits in surface characterization, such studies leave several questions unanswered. First, in the study of complex catalytic materials, these techniques yield ensemble results, averaged over Avogadro numbers. It is not straightforward to extract from these results the precise contribution of the different surface groups or metal species one observes. Secondly, in many studies, attention is devoted to unravelling the spectroscopic fingerprints of the inorganic species on the catalyst surface. While the observed surface species may be the actual active sites, one may also observe species or functional groups that are formed during the reaction but do not actively participate in the actual reaction, *i.e.* spectator species. Thirdly, the fate of adsorbed organics, such as reagents or reaction products, should be monitored simultaneously, but many techniques lack the specificity to follow transformations of single bonds in complex organic molecules. More specialized approaches, like sum frequency generation spectroscopy, are required to address reactivity of organics at catalytic surfaces. A final problem encountered with ensemble spectroscopic techniques is quantification, since it is hard to determine appropriate extinction coefficients.

A major step forward was the introduction of high resolution microscopes, such as scanning probe microscopy and electron microscopy. These instruments can directly observe and quantify metal atoms and adatoms on surfaces. Scanning probe techniques are however typically limited to single, idealized crystals in ultrahigh-vacuum conditions (UHV), and

* Corresponding author. Tel.: +32 16 321593; fax: +32 16 321998.
E-mail address: bert.sels@biw.kuleuven.be (B.F. Sels).

0920-5861/$ – see front matter
doi:10.1016/j.cattod.2007.03.007

the discrepancy between such conditions and industrial catalysis ('pressure gap', 'materials gap') has been debated increasingly in the past years. The '*pressure gap*' refers to the difference between the UHV conditions of classical surface science ($<10^{-9}$ bar) and the pressures in industrial applications (1 to 10^{3} bar). At least regarding scanning tunnelling microscopy (STM), the gap has considerably been narrowed over the last decade. The example of CO oxidation on Ru(0 0 0 1) eloquently illustrates the 'pressure gap' [1]. In UHV conditions, Ru shows by far the poorest catalytic activity of the Pt group metals, but it turns out to be superior to Pt and Pd if operated in excess of oxygen at atmospheric pressure. Originally it was thought that this reversal was due to formation of a complete monolayer of chemisorbed oxygen, but STM studies after exposure to 10^{-5} bar of gaseous O_2 showed that the real active phase is epitaxially grown RuO_2(1 1 0). Higher pressures of >1 bar were used in an STM study of the CO oxidation on Pt(1 1 0) [2]. In vacuum (<0.2 bar), the CO oxidation on the metal surface follows Langmuir–Hinshelwood kinetics, with a surface reaction between CO and oxygen. However, at higher O_2 pressures, surface oxides are formed, and the reaction follows a Mars–Van Krevelen mechanism [3]. Such studies show that upon reagent adsorption, STM can address the dynamics of solid surfaces, such as reconstruction, surface alloying and oscillatory behaviour. The large impact of minor environmental changes on the inorganic surface convincingly illustrates the need to approach real reaction conditions as closely as possible.

The *'materials gap'* refers to the distinction between the idealized flat single crystals of surface science and the real catalysts, containing *e.g.* metal particles of nanodimensions and with curved surfaces in a porous matrix. It is often suspected that sites with low coordination number, *e.g.* defect sites and surface atoms on edges and kinks, have a much stronger influence on the catalytic behaviour than smooth crystal planes. This has been effectively proven by STM using models of gradually increasing complexity, *e.g.* Au doped onto Ni(1 1 1), or Co-doped MoS_2 crystals grown on Au(1 1 1) [4]. However, as STM is only able to deal with conductive surfaces, and as the instrumental stability requires flat substrates, it seems unfeasible to study particles supported in porous, irregular and often insulating supports. Nevertheless, many important heterogeneous catalysts have a three-dimensional porous structure, with the reaction taking place inside the pores, and with pore confinement controlling the selectivity. Additionally, several groups of catalysts do not contain supported clusters or functions, but have intrinsically active lattices, and such materials are not amenable to the design of simplified model systems on flat substrates.

A third gap that can be identified is the '*phase gap*'. Indeed, all previous examples focus on reactions between gaseous phase reagents and a solid surface. Even in catalysis for base chemicals production, the current trend is definitely towards condensed phase catalysis. Liquid phase reactions, for instance using zeolites, operate in conditions of complete pore filling, and this can be exploited to increase selectivity and catalyst longevity, as in ethylbenzene synthesis. For many fine chemical transformations, there is no alternative to liquid phase operation, since the molecules are insufficiently stable to be volatilized. Few, if any techniques can monitor *in situ* condensed phase reactions in porous or non-conducting catalysts. The 'phase gap' becomes all the more critical considering the complexity of solvent effects in heterogeneously catalyzed reactions, including surface phenomena such as competitive adsorption.

While physical studies in the condensed phase are unusual to catalytic science, they are more familiar to biologists, since cellular processes are occurring in the liquid phase. One of the most powerful techniques in biological research is fluorescence microscopy, including recent evolutions in single molecule spectroscopy (SMS). SMS is a rapidly expanding research area, and some excellent reviews are available [5–8]. In the next paragraphs, some of the essentials of fluorescence microscopy and single molecule fluorescence spectroscopy will be highlighted, together with some applications in biology. The potential application of fluorescence spectroscopy to the study of catalytic materials will be discussed, and it will be demonstrated that many of the previously discussed needs of current catalytic research, including the phase and materials gaps, can be addressed using fluorescence microscopy. This will be illustrated with some new data on the visualization of a catalytic reaction in the pores of a mordenite zeolite.

2. Single molecule fluorescence microscopy and spectroscopy

As a first requirement to single molecule fluorescence microscopy and spectroscopy, the fluorescence intensity of the molecule should be well above the background. This background can originate from inelastic scattering and from impurity fluorescence in the used solvents, coverslips, optics and of course from the dark counts generated by the detector. The first successful single molecule fluorescence measurements date back to the early 1990s, and were performed at cryogenic temperatures to increase the absorption and fluorescence probability [9,10]. These measurements were quickly followed by the first studies of single molecules at room temperature. The original near field approach has been often used in the following years [11–14], but eventually far field microscopes proved easier to operate [15–18]. The two commonly used far field setups are the confocal and widefield microscope (see Fig. 1). In the first setup the objective lens focuses the excitation light to a diffraction-limited spot. Before reaching the detector, the fluorescence light passes a pinhole, rejecting the out of focus light. The fluorescence intensity can be measured by a point detector (avalanche photodetector, APD; photomultiplier tube, PMT) which very efficiently detects photons with a low dark current, resulting in a good signal-to-noise ratio (SNR). These measurements with a microsecond temporal resolution can determine fluorescence lifetimes at a subnanosecond time scale. Emission spectra can be measured with a CCD camera combined with a polychromator. With the confocal technique one molecule is studied at a time, and imaging of extended areas is possible by scanning

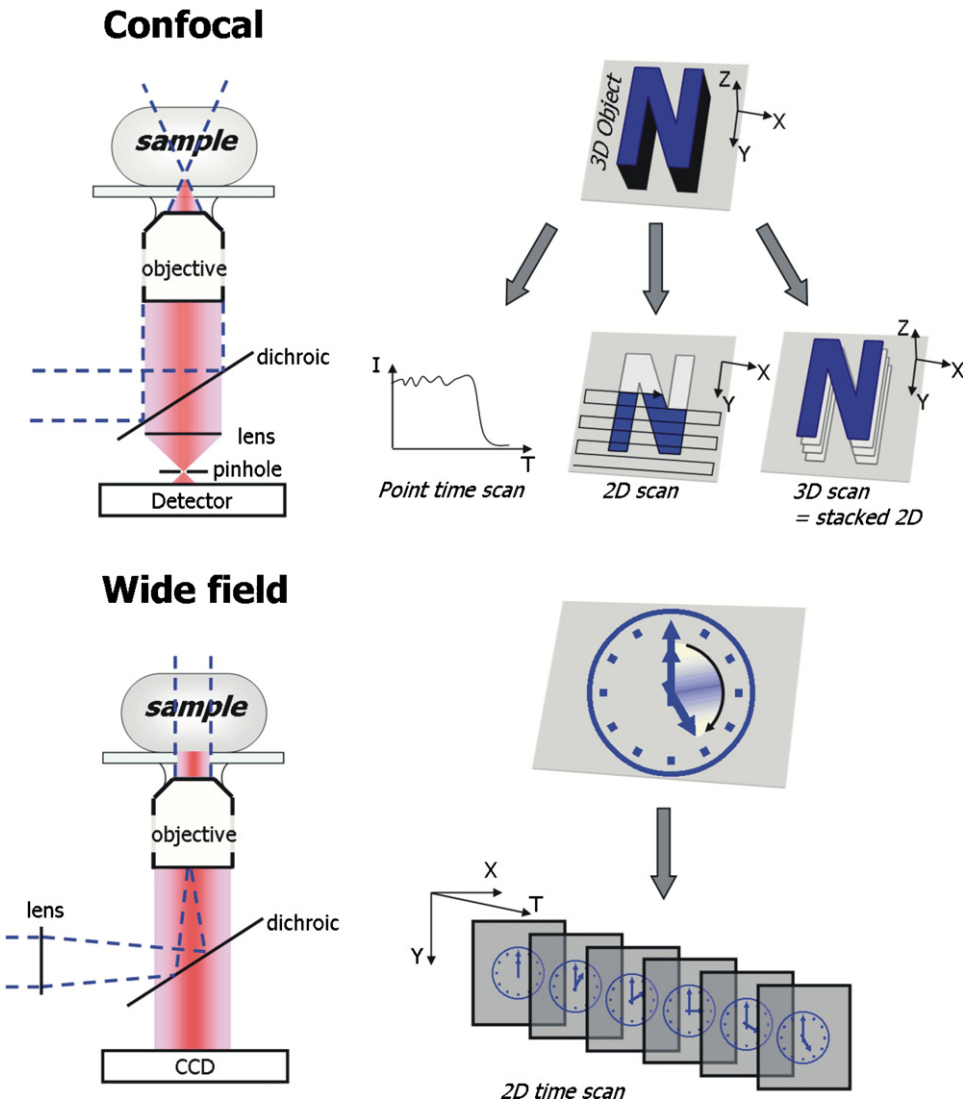

Fig. 1. Fluorescence microscopy setups. In the *confocal* approach, the collimated excitation light from the source is reflected by the dichroic mirror onto the objective lens. By overfilling the back aperture the light is then focused into a small spot. The fluorescence light is collected by the same objective lens and is transmitted by the dichroic mirror. In the *widefield* setup the collimated laser light is focused with a lens on the back aperture of the objective lens giving a collimated light beam illuminating the sample. The fluorescence generated by this area is then collected by the objective and passed through the dichroic mirror before touching the CCD camera.

the sample with respect to the laser or vice versa. As a consequence of the single molecule sensitivity, analytical details such as fluorescence intensity, decay time and emission spectra of individual molecules can be collected. This approach is mainly useful to get highly temporally resolved dynamic data on individual molecules. Due to its small femtoliter excitation volume, the confocal technique is suitable for studying structures in three dimensions.

In widefield microscopy a CCD camera is used to film events taking place in the several hundred square micrometers large excitation area. The resolvable spots are again diffraction-limited, but now represent a larger excitation volume due to a decreased resolution in the *Z*-direction, reducing the SNR. The time resolution for large domain imaging is limited by the frame transfer rate of the used CCD camera (millisecond range) and is lower than for the aforementioned point detectors. On the other hand several molecular events can be monitored at the same time and by appropriate fitting of the point spread function (PSF), molecules can be localized with a precision far below the diffraction barrier [19]. Working with total internal reflection illumination implies excitation by an evanescent field, as is also done in ATR-IR spectroscopy; the reduced excitation volume results in an increased SNR. Widefield microscopes are most commonly used to study diffusion and other dynamic processes taking place over an extended area. Accordingly, rotational behaviour/freedom of individual molecules has been investigated using polarized detection in confocal or widefield microscopy or using defocused widefield imaging [20,21]. Some enzymatic or cellular examples will show the strength of SMS and clarify the differences between the confocal and the widefield approaches.

Since most enzymatic reactions occur at time scales of milliseconds to seconds, the confocal approach is most suited to study the fastest enzymes, while enzymes with lower rates (<40 frames/s) can also be studied with a widefield approach [22,23]. SMS studies have recognized both dynamic and static disorder in enzymatic action. The static disorder, *i.e.* the variation of the activity of individual enzymes within a population, has been demonstrated with capillary electrophoresis by looking at the fluorescence of NADH, accumulated by single molecules of lactate dehydrogenases over longer time periods [24]. While the latter work did not actually observe single turnovers, this aim was achieved using cholesterol oxidase in a confocal microscope [25]. Cholesterol oxidase uses a fluorescent flavine cofactor to shuttle electrons to O_2; while FAD is fluorescent, its reduced state $FADH_2$ is not. By diluting one single enzyme in the excitation beam and monitoring the ON–OFF fluorescence signal and observing single catalytic turnovers, dynamic disorder in enzymatic action could be proven. This means that a single enzyme has a time-dependent activity; short bursts of activity alternate with longer resting periods.

One of the practical difficulties of fluorescence microscopy could be photobleaching of the chromophore. One solution is to work with fluorogenic substrates. These substrates are non-fluorescent in their native form and only after catalytic cleavage fluorescent products are formed [26,27]. Since photobleaching is no longer the limiting factor, this approach allows SM turnovers to be monitored for several hours on one individual enzyme. Even though kinetics at a single molecule level show fluctuations complicating the ensemble Michaelis–Menten kinetics, this behaviour over longer periods averages out to the same simple kinetics, as postulated by the ergodic principle [28].

As an application of widefield fluorescence microscopy in the study of single molecule enzyme dynamics, the stepwise movement of labelled motor proteins like myosin and kinesin has been nicely monitored [29,30]. These proteins are capable of transforming chemical energy from adenosine triphosphate (ATP) into mechanical movement [31]. Although step sizes are much smaller than the diffraction limit, determination of the centre of the point spread function (PSF) allows nanometer-precise positioning of the chromophore. This direct visualization proved the 'hand-over-hand' model, in which the two heads of the kinesin motor enzyme alternately take the front position while the kinesin moves over the microtubuli. With a similar approach the infection of individual, micrometer-sized cells by single, nanometer-sized adeno-associated virus particles could be monitored [32].

Other fluorescence microscopy related techniques have been applied in biological research to study microscopic dynamics [33], such as fluorescence correlation spectroscopy (FCS) [34–36], fluorescence resonance energy transfer (FRET) [37,38], fluorescence lifetime imaging microscopy (FLIM), or fluorescence recovery after photobleaching (FRAP). Recent technical advances have concentrated on increasing the resolution of confocal fluorescence microscopy at least with one order of magnitude by for example working with stimulated emission depletion microscopy [39]. This approach has been used recently to monitor the fate of 40 nm vesicles inside a cell [40].

3. Fluorescence microscopic studies of catalytic materials

Next to applications in biological research, fluorescence microscopy also proved its power in materials research. Polymers and their dynamics are a preferred study object. With single molecules the void spaces can be probed [41], the diffusional and rotational freedom directly studied and the processes at the glass transition can be investigated [21,42]. In some cases single molecules have been visualized at elevated temperatures up to 373 K [43,44] showing that the technique is not limited to ambient temperature.

Fluorescence and fluorescent molecules have received considerable attention in studies of molecular sieves and other potentially catalytic materials like clays. Generally, the focus has been on supramolecular organization, and on control of the photophysical and photochemical properties of guest molecules, instead of on surface reactivity [45–47]. Molecules can be aligned in zeolites with one- or two-dimensional pore systems, and depending on size restrictions, they can be admitted into or excluded from the inner pore volume. Packing or confinement effects in channels and cages, or interactions with pore walls and exchanged cations can control aggregation of chromophores, their lifetimes and quantum yields, and energy or electron transfer phenomena between guest molecules.

In most of the previous studies on solid materials, bulk measurements have been performed on such materials, and only properties averaged over all crystals in the sample and all sites within the crystal are measured. In a few cases, however, improved temporal and especially spatial resolution has been employed to monitor the heterogeneity of elementary phenomena such as diffusion within a macroscopic sample. While the resolution is essentially diffraction-limited, one may also use large crystals of zeolites or clays. It can be safely assumed that such crystals present similar site heterogeneity as smaller entities, and they are much more suitable as a study object.

3.1. Sorption and diffusion in zeolites and other porous molecular sieves

Intercrystalline diffusion between zeolite X crystals in a powder sample has been probed using chrysene or perylene as a guest and NaX or TlX zeolites as hosts [48–50]. In a physical mixture of chrysene-loaded NaX and unloaded TlX, one can easily determine the location of the chrysene: chrysene gives a blue fluorescence in NaX, but in TlX, a green phosphorescence is seen, because of spin-orbit interaction with Tl^+ cations. By manipulating the particles in the microscope, close contact between the 2–3 μm chrysene-loaded NaX and unloaded TlX crystals can be induced, and the gradual migration of the chrysene can be followed in real time. Such experiments showed moreover that upon loading of a powder sample with an

aromatic compound, the dye content of the individual crystallites may strongly vary, because of the slow diffusion of the aromatics in the dry sample.

Provided that the molecular sieves consist of very large crystals, fluorescence microscopy can visualize heterogeneities within a single crystal. Using large crystals of silicalite (length > 60 μm) or AlPO-5 (length > 300 μm), the cracks and defects formed upon calcination have been visualized by loading with dyes that are normally too large to enter the pore system in a regular fashion [51]. Similarly, uptake of a stilbene dye in a single 300 μm particle of a M41S mesoporous molecular sieve has been monitored.

Zeolites with LTL topology usually have much smaller crystals, and special techniques are required for observing intracrystalline diffusion via fluorescence imaging. L-zeolites have a well-accessible, one-dimensional pore system, and this makes them excellent hosts for dye organization [46]. Properly selected dyes cannot glide past each other in the 7.3 Å channels, and this allows for preparation of 'sandwich' materials, by consecutive insertion of the dyes in the channels. This results in zoning of the dyes within the crystal, which can be visualized, even for 1 μm crystals, by selective excitation and detection at well-chosen wavelengths. For example, consecutive loading of L-zeolite with an oxonine (Ox^+), with 2,2′-*p*-phenylenebis(4-methyl-5-phenyloxazole) (DMPOPOP), and finally a pyronine (Py^+) results in intrachannel location of Ox^+, while the DMPOPOP closes the channel mouths in a stopcock-like fashion (Fig. 2). Finally the Py^+ is localized on the outer surface. This spatial heterogeneity was mapped using three different excitation wavelengths, and, if appropriate, transmitting only the emission polarized in the direction of the crystal axis.

More quantitative information can be gained by simultaneously loading the L-zeolite with a mixture of Py^+ and Ox^+ [52]. Initially the dyes are close to each other. Upon excitation of the Py^+ donor, energy transfer to the Ox^+ acceptor is fast, and red emission from Ox^+ is generated. After diffusion of the dyes throughout the channels, the average distance between Ox^+ and Py^+ is increased, and the rate of energy transfer decreases. From the emission ratio I_{Ox^+}/I_{Py^+}, intracrystalline diffusion coefficients in the order of 10^{-20} m^2 s^{-1} have been determined.

Single molecule tracking constitutes an even more direct approach to the determination of diffusion constants. In pioneering work, Bräuchle and co-workers followed the motion of terrylenediimide, encapsulated during the synthesis in a (non-calcined) M41S material [53]. Analysis of the trajectories of individual molecules showed that two subpopulations could be distinguished: 10% of the molecules are almost stationary, while 90% of the molecules move with 0.1–1 μm steps per 4 s between the images. From the frequency distribution of the mean square displacements, D was evaluated at 3.7×10^{-14} m^2 s^{-1}. Despite the channel-structure of M41S, motional anisotropy could not be observed, possibly because of too low spatial (40 nm) or temporal (4 s) resolution of the experiment. Similar D values were determined for other dye molecules in mesoporous materials based on the same method [54,55]. Using a similar system, *viz*. Nile red in a mesoporous silica thin film, a different approach was followed for determining the diffusion constants [56]. Single point fluorescence transients, recorded for over 1 h in wet films, display on–off behaviour which is related to the diffusion of individual dye molecules into and out of the focal volume. Longer 'on' periods can be ascribed to adsorption of Nile red on the siliceous surface. Using the appropriate autocorrelation function for two-dimensional diffusion and allowing for adsorption, a D value of 2.5×10^{-14} m^2 s^{-1} was obtained, with typical desorption times $1/k$ of 25–40 s.

The orientation of single dye molecules, *e.g.* oxazines in AlPO-5, was assessed by inserting a rotating broad band λ/2 plate into the setup, in order to modulate the polarization plane of the excitation light [57]. At extreme dye dilution, about 10 molecules can be evaluated for each crystal of 10 μm length. For sufficiently slender molecules in the one-dimensional

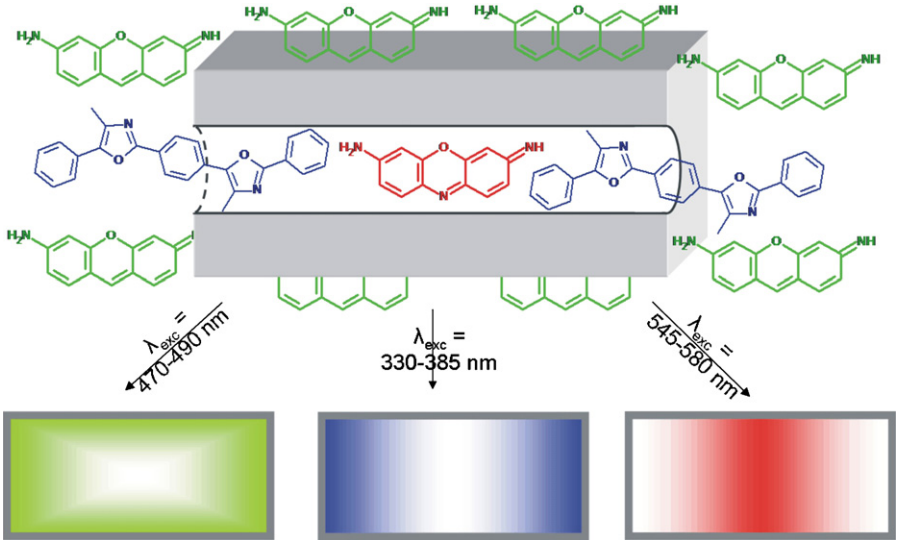

Fig. 2. Localization of dyes in the pores of micrometer-sized zeolite L-crystals. The Ox^+ dyes inside the channels give a red fluoresence; the DMPOPOP molecules at the pore entrances give blue fluorescence, and the green-emitting Py^+ dyes occupy the outer surface [41]. (For interpretation of the references to colour in this figure legend, the reader is referred to the web version of the article.)

pores, there is only a limited deviation from the average orientation along the main crystal axis.

3.2. Sorption, diffusion and catalysis in layered materials

Some studies have been devoted to uptake of anionic dyes on layered double hydroxides (LDHs). These materials, also known as hydrotalcite-like materials, contain a net positive charge in their brucite-like layers due to isomorphous substitution, and hence charge compensating anions are located in between the sheets or at the outer surface [58].

For phenolphthalein in a Zn,Al-containing LDH, inhomogeneous distribution of the dye over the particles could be observed [59]. However, due to the small size of the crystallites (~5 μm), and due to aggregation of these crystallites, it proved difficult to identify the precise cause of such inhomogeneities. Better resolved pictures were obtained using Li,Al-LDHs [60]. These materials are obtained as large, flat hexagonal crystallites with a 20–30 μm diameter. Time-resolved observation of the uptake of a carboxylated perylene imide (PMI-COOH) on these crystals shows that the anion exchange starts at the side planes of the LDH crystals. This initial uptake is followed by slower diffusion over the basal plane. Modelling of the time-dependent intensity in different zones of the crystal resulted in a value of $D = 3\text{–}3.7 \times 10^{-14}$ m^2 s^{-1}. The PMI-COO$^-$ anions can be readily displaced by carbonate anions, with an apparent time constant $1/k$ of 25 s.

The basic catalytic properties of LDHs were explored in a recent *in situ* study by our team [61]. LDHs may exhibit basic sites either on the basal planes, *viz.* the structural hydroxide groups, or at the crystal fringes, *viz.* exchanged hydroxyl anions. As a pro-fluorescent reagent, we used fluorescein esters such as fluorescein diacetate (FDA). These can be converted to fluorescein either by hydrolysis in an aqueous medium, or by transesterification in an alcohol solvent. Upon addition of FDA to an LDH crystal in butanol, bright spots appear all over the basal plane. These spots are due to single molecules of fluorescein. Before photobleaching, they can be seen walking over the surface, and the step sizes of their trajectories can be analyzed. The population of product molecules contains, besides a majority of mobile molecules ($D = 3 \times 10^{-14}$ m^2 s^{-1}), a small number of almost immobile molecules. A totally different picture is obtained when FDA is hydrolyzed on LDHs. In this case, at least 85% of the product spots are formed at crystal edges. This example shows that the spatiotemporal resolution of the technique is sufficient for ascribing different catalytic activities to different zones and sites within the catalytic crystal. While structure-sensitive catalysis has previously been monitored in gas phase reactions [62], fluorescence microscopy is the first technique to directly and unambiguously determine such phenomena in the condensed phase.

4. Towards imaging of molecular catalysis inside porous frameworks

The previous part discussed studies of inter- and intraparticle diffusion in zeolites, and of diffusion and single molecule catalysis on layered materials. In contrast to many surface science spectroscopic techniques, fluorescence microscopy is capable of studying diffusion and catalysis in zeolite pores with high 3D spatial and temporal resolution [63]. In the following examples, fluorogenic probes are chosen that are smoothly transformed into fluorescent molecules upon chemical transformation. These fluorescent molecules are either typical reaction intermediates, such as carbocations, or reaction products.

After deposition of the calcined zeolite on a glass coverslip the sample was placed in a sample holder specially designed for microscopic studies (see Fig. 3). In this liquid cell facility, the substrate can be added to the used solvent (for more details see Section 6). In a first example, we studied the oligomerization of furfuryl alcohol on an acid mordenite (H-MOR). Furfuryl alcohol oligomerization starts with alkylation of one furfuryl alcohol molecule by another in an electrophilic aromatic substitution (EAS). After some subsequent acid-catalyzed

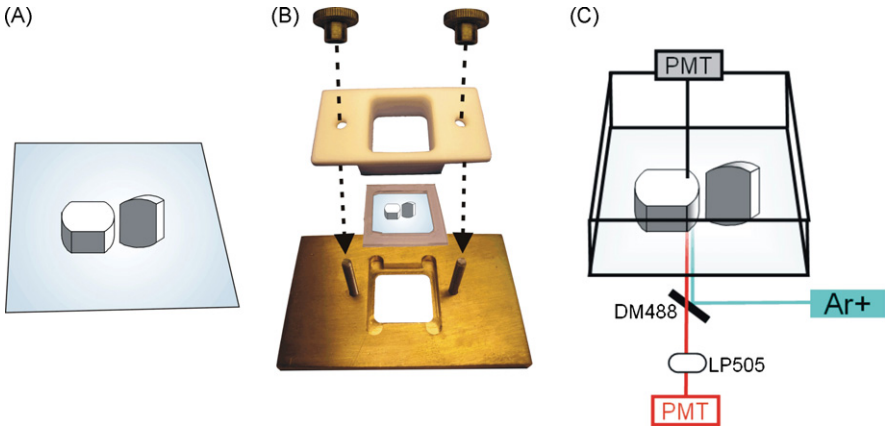

Fig. 3. (A) For the microscopic experiments, the zeolite crystals were deposited on freshly cleaned coverglass via spincoating from a dispersion in *n*-butanol. (B) The coverglass is placed into a specially designed sample holder (3 ml volume). The solvent can be added into a teflon container which is pressed using a silicone rubber sealing onto the coverglass. (C) This small batch reactor can be directly used in a standard epi-fluorescence microscope. In this setup, the light from an Ar^+ laser (488 nm) is directed via a dichroic mirror (DM) onto the sample. The transmission image is collected with one photomultiplier tube (gray PMT) whereas the generated fluorescence signal is collected using a second photomultiplier tube (red PMT) using a 505 nm long pass filter. (For interpretation of the references to colour in this figure legend, the reader is referred to the web version of the article.)

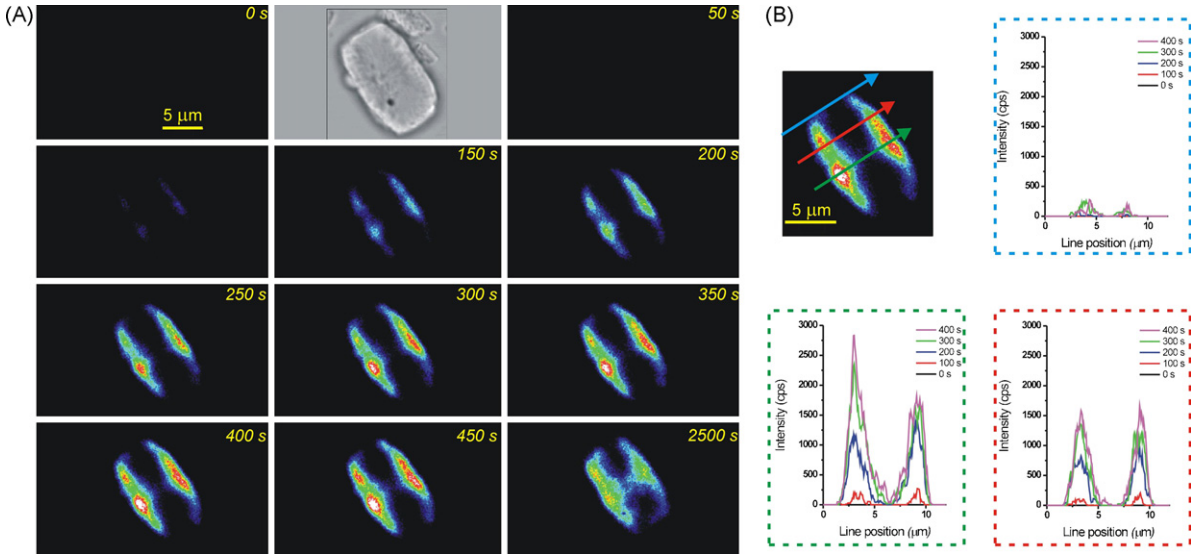

Fig. 4. Visualization of the furfuryl alcohol self-reaction in a mordenite crystal. (A) The reaction is monitored as a function of time (false color images). The inset shows an optical transmission image of the same catalytic crystal in grayscale. (B) The fluorescence intensity along three selected lines (blue, red and green) parallel to the [0 0 1] direction as a function of time (For interpretation of the references to colour in this figure legend, the reader is referred to the web version of the article.).

reaction steps, a family of fluorescent compounds is formed [64]. Fig. 4 visualizes the fluorescence development after the zeolite was contacted with a diluted solution of furfuryl alcohol in *n*-BuOH. Fluorescence time-lapse measurements (Fig. 4B) clearly show the evolution of catalytic activity from two opposing crystal faces, while no light is emitted from the rest of the outer zeolite surface. Transmission images evidence that the reactive crystal faces are the (0 0 1) planes. As the reaction carries on, fluorescence propagates along the [0 0 1] direction, corresponding to the 12-membered ring channels in mordenite. As furfuryl alcohol is too large to access the 8-membered ring pores, no fluorescence develops from the other faces of the

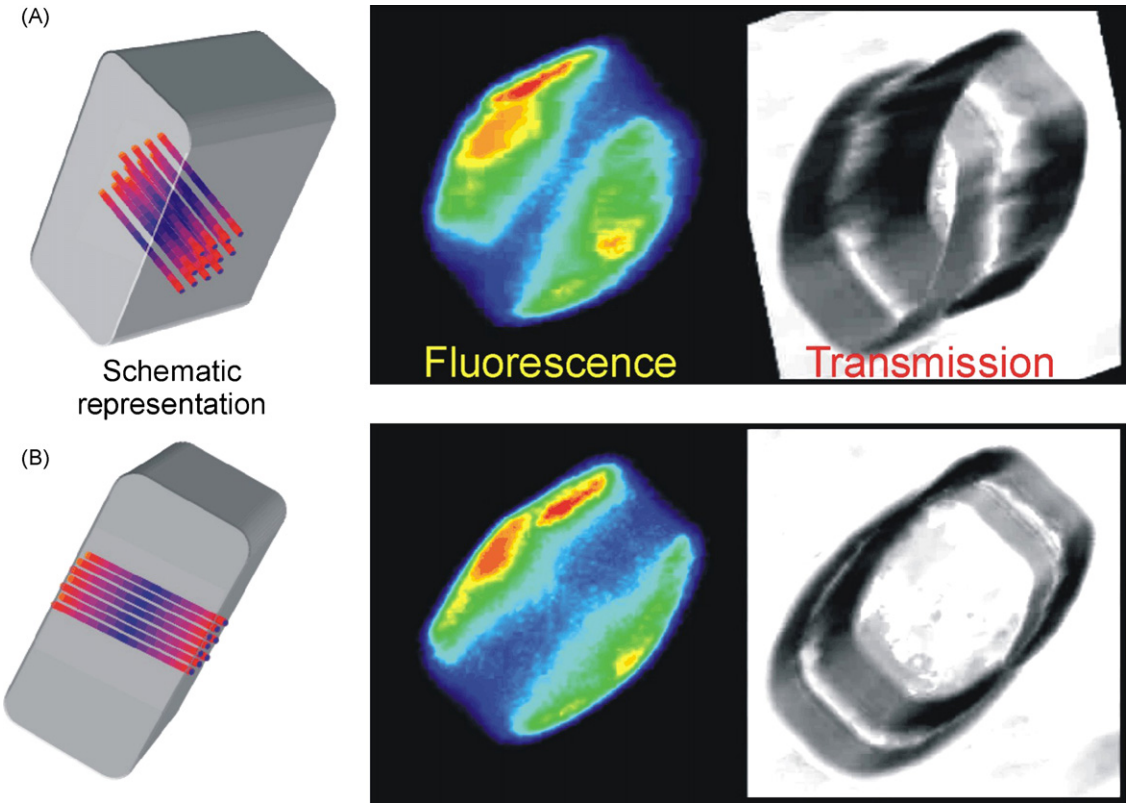

Fig. 5. Three-dimensional visualization of acid-catalyzed furfuryl alcohol oligomerization in a mordenite crystal under different viewing angles (A and B). For each orientation a schematic representation of the crystal is given along with the corresponding fluorescence and transmission images.

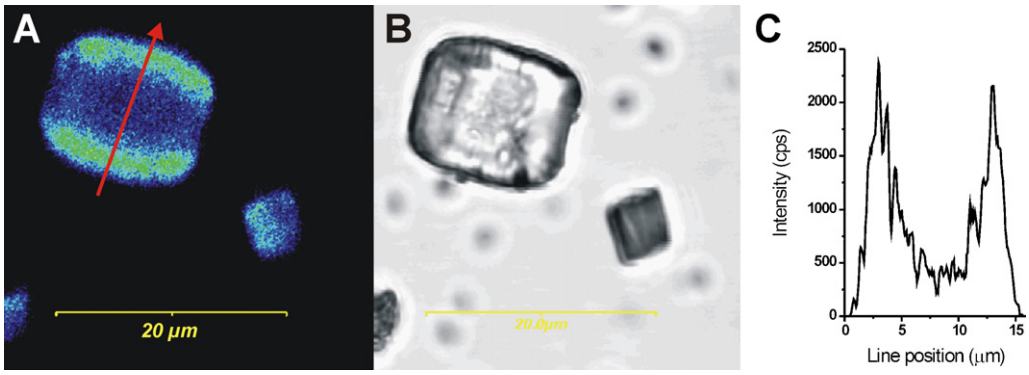

Fig. 6. Reactive zones inside a mordenite crystal during dehydration of 1,3-diphenyl-1,3-propanediol. For conditions, see Section 6. (A) False color fluorescence image, (B) transmission image, and (C) line profile of the fluorescence intensity along the line indicated in (A).

crystal. The spatial resolution is sufficient to monitor the fluorescence intensity at any point in the crystal, for instance, by scanning through the crystal along the [0 0 1] direction (Fig. 4B). The figure clearly shows the gradual formation of fluorescent molecules and the evolution of the fluorescence along the crystals 12 ring pores from the outer surface to the crystal interior. The fluorescence intensity along the red and green line shows a comparable behaviour with a slightly higher concentration of catalytic activity in the central part of the crystal, whereas the catalytic activity along the blue line (near the edge of the crystal) is very small even at longer times. This implies inaccessibility of the crystal interior from faces other than (0 0 1). In Fig. 5 a three-dimensional image of the catalytically active zones inside a mordenite crystal is shown. Such 3D visualizations are generated by volume processing of individual image stacks consisting of consecutive scans along the optical path, *i.e.* the microscope's *Z*-axis. Thus, fluorescence microscopy permits to accurately visualize this acid-catalyzed self-condensation on a single catalyst crystal, with an unprecedented sensitivity and spatiotemporal resolution.

In another example, we followed the acid-catalyzed formation of a stable carbocation inside the zeolite structure. Fig. 6 summarizes the results obtained for the dehydration of 1,3-diphenyl-1,3-propanediol. The carbocation formed upon dehydration fluoresces with high efficiency due to rotation and translation restrictions in the zeolite channels [65]. Specific visualization of these carbocations directly shows the locus of catalytic activity as can be seen in Fig. 6A. For these measurements, similar zeolite crystals were used as in Figs. 4 and 5. The fluorescence evolution again indicates that the active sites of these mordenite zeolite crystals can be accessed from the two (0 0 1) crystal faces. A line scan of the fluorescence intensity (Fig. 6C) shows the highest catalytic activity near the pore entrances. The same line scan also suggests the formation of fluorescent carbocations in the central part 5–8 μm away from the outer surface which may be taken as proof for the effective diffusion of large aromatic reagent molecules inside the 12-ring pores.

With other currently used methods, it is – to the best of our knowledge – impossible to obtain such spatially detailed *in situ* information on acid zeolite catalysis. Accordingly, other zeolite-related issues, such as morphology dependent zeolite catalysis, pore mouth catalysis, etc. can be addressed now using fluorescence microscopy. Recently a similar study by our groups has shown the impact in terms of diffusion barriers of the hourglass-shaped compartmentalization in ZSM-5 crystals on their catalytic activity [63].

5. Conclusion

The new data in this paper, and the cited literature examples show the potential of fluorescence microscopy as an *in situ* characterization technique in heterogeneous catalysis. Like in biology, fluorescence microscopy can be used to study processes in the condensed phase, thus effectively bridging the phase gap. However, there is no objection against application of the technique in the gas phase. The spatiotemporal resolution and sensitivity cannot be matched by many other spectroscopic techniques. This makes it possible to probe and localize active regions within catalyst particles, to follow inter- and intraparticle migration or reagent transformation, to study kinetics of small domains or even single active sites, and to determine the release of organic molecules from inorganic hosts [66]. Such insights cannot only be used for the development of more efficient catalyst particles, but also in the design and evaluation of drug delivery systems or other devices.

Besides imaging, fluorescence microscopy can also gather other data such as decay times, intensity fluctuations, emission spectra, . . ., even at the single molecule level. From these data, dynamic changes in the nanoenvironment can be probed with a submillisecond resolution. While the currently achievable spatial resolution might still be problematic for the study of nanometer sized objects, recent technical evolutions, such as STED, are steps towards overcoming this problem. Even if current work on fluorescence in catalysis is still very limited, it can be expected that the synergy with the use of fluorescence in biological research will result in an explosion of new insights in the coming years.

6. Experimental

6.1. Materials

The mordenite catalyst (H-MOR, ZM-980) was acquired from Zéocat (Montoir de Bretagne, France). It has a Si/Al ratio

of 100; the crystals typically have dimensions of 10–20 μm. Before use in the microscopic experiments, the mordenite crystals were thermally activated under air. First, the sample was heated at 5 °C min^{-1} to 120 °C and kept at this temperature for 3 h, in order to remove physisorbed water. This treatment prevents hydrothermal destruction of large crystals. Next, the samples were further heated to 520 °C (5 °C min^{-1}) and kept at this temperature for 24 h. The samples were cooled down and stored under dry nitrogen in a desiccator for maximally 1 week.

6.2. Laser scanning confocal microscopic experiments

The measurements were performed on an Olympus FluoView™ 500 (Olympus, Tokyo, Japan) confocal laser scanning fluorescence microscope, in which the fluorescence intensity was combined with observation of the optical transmission image. For this an Ar^+ laser (Spectra Physics, Mountain View, CA, USA) giving continuous excitation at 488 nm was directed via two scanning galvano mirrors on the sample using an oil immersion objective lens (Olympus, 100×, 1.4 NA) yielding an excitation power of 23 μW on the sample. The fluorescence signal is separated through a 488 nm dichroic mirror and a 505 nm long pass filter (Chroma Technology, Rockingham, VT, USA) before it reaches the photomultiplier tube. Two- and three-dimensional measurements are standard scanning modes readily available via the microscope's operating system. Further analysis was also performed with this same software.

6.3. Furfuryl alcohol oligomerization [64]

The mordenite crystals are dispersed in *n*-butanol before deposition on cleaned coverglasses by spin coating (1000 rpm, 60 s). In the microscopic experiments, these catalyst-loaded coverglasses are submerged in 980 μl of the reaction solvent *n*-butanol, to which a 20 μl aliquot of furfuryl alcohol is added (see Fig. 3).

6.4. Acid-catalyzed dehydration [65]

This reaction was conducted in a similar way, by exposing the mordenite to a 8.75×10^{-5} M solution of 1,3-diphenyl-1,3-propanediol in dichloromethane. 1,3-Diphenylpropanediol was obtained by $NaBH_4$ reduction in ethanol of commercial 1,3-diphenyl-1,3-propanedione (Aldrich, Schnelldorf, Germany).

Acknowledgements

M.B.J.R. thanks the Institute for the Promotion of Innovation through Science and Technology in Flanders (IWT-Vlaanderen) for a fellowship. G.D.C. wishes to thank F.W.O. (Research Foundation Flanders) for financial support. This work was performed within the framework of the IAP-V-03 programme 'Supramolecular Chemistry and Catalysis' of the Belgian Federal government and of GOA-2/01. We also gratefully acknowledge support from the K.U. Leuven in the frame of the Centre of Excellence CECAT.

References

[1] H. Over, Y.D. Kim, A.P. Seitsonen, S. Wendt, E. Lundgren, M. Schmid, P. Varga, A. Morgante, G. Ertl, Science 287 (2000) 1474.
[2] B.L.M. Hendriksen, S.C. Bobaru, J.W.M. Frenken, Top. Catal. 36 (2005) 43.
[3] P. Mars, D.W. van Krevelen, Chem. Eng. Sci. 3 (1954) 41.
[4] J.V. Lauritsen, R.T. Vang, F. Besenbacher, Catal. Today 111 (2006) 34.
[5] X.S. Xie, J.K. Trautman, Annu. Rev. Phys. Chem. 49 (1998) 441.
[6] A.A. Deniz, T.A. Laurence, M. Dahan, D.S. Chemla, P.G. Schultz, S. Weiss, Annu. Rev. Phys. Chem. 52 (2001) 233.
[7] F. Kulzer, M. Orrit, Annu. Rev. Phys. Chem. 55 (2004) 585.
[8] P. Tinnefeld, M. Sauer, Angew. Chem. Int. Ed. 44 (2005) 2642.
[9] W.E. Moerner, L. Kador, Phys. Rev. Lett. 62 (1989) 2535.
[10] M. Orrit, J. Bernard, Phys. Rev. Lett. 65 (1990) 2716.
[11] E. Betzig, R.J. Chichester, Science 262 (1993) 1422.
[12] J.K. Trautman, J.J. Macklin, L.E. Brus, E. Betzig, Nature 369 (1994) 40.
[13] W.P. Ambrose, P.M. Goodwin, J.C. Martin, R.A. Keller, Phys. Rev. Lett. 72 (1994) 160.
[14] X.S. Xie, R.C. Dunn, Science 265 (1994) 361.
[15] J.K. Trautman, J.J. Macklin, Chem. Phys. 205 (1996) 221.
[16] J.J. Macklin, J.K. Trautman, T.D. Harris, L.E. Brus, Science 272 (1996) 255.
[17] H.P. Lu, X.S. Xie, Nature 385 (1997) 143.
[18] X.S. Xie, Acc. Chem. Res. 29 (1996) 598.
[19] M.K. Cheezum, W.F. Walker, W.H. Guilford, Biophys. J. 81 (2001) 2378.
[20] J.N. Forkey, M.E. Quinlan, M.A. Shaw, J.E.T. Corrie, Y.E. Goldman, Nature 422 (2003) 399.
[21] H. Uji-i, S.M. Melnikov, A. Deres, G. Bergamini, F. De Schryver, A. Herrmann, K. Mullen, J. Enderlein, J. Hofkens, Polymer 47 (2006) 2511.
[22] H. Engelkamp, N.S. Hatzakis, J. Hofkens, F.C. De Schryver, R.J.M. Nolte, A.E. Rowan, Chem. Commun. 9 (2006) 935.
[23] X. Michalet, S. Weiss, M. Jaeger, Chem. Rev. 106 (2006) 1785.
[24] Q.F. Xue, E.S. Yeung, Nature 373 (1995) 681.
[25] H.P. Lu, L.Y. Xun, X.S. Xie, Science 282 (1998) 1877.
[26] O. Flomenbom, K. Velonia, D. Loos, S. Masuo, M. Cotlet, Y. Engelborghs, J. Hofkens, A.E. Rowan, R.J.M. Nolte, M. Van der Auweraer, F.C. de Schryver, J. Klafter, Proc. Natl. Acad. Sci. U.S.A. 102 (2005) 2368.
[27] K. Velonia, O. Flomenbom, D. Loos, S. Masuo, M. Cotlet, Y. Engelborghs, J. Hofkens, A.E. Rowan, J. Klafter, R.J.M. Nolte, F.C. de Schryver, Angew. Chem. Int. Ed. 44 (2005) 560.
[28] B.P. English, W. Min, A.M. van Oijen, K.T. Lee, G. Luo, H. Sun, B.J. Cherayil, S.C. Kuo, X.S. Xie, Nat. Chem. Biol. 2 (2006) 87.
[29] A. Yildiz, M. Tomishige, R.D. Vale, P.R. Selvin, Science 303 (2004) 676.
[30] A. Yildiz, J.N. Forkey, S.A. McKinney, T. Ha, Y.E. Goldman, P.R. Selvin, Science 300 (2003) 2061.
[31] R.D. Vale, T. Funatsu, D.W. Pierce, L. Romberg, Y. Harada, T. Yanagida, Nature 380 (1996) 451.
[32] G. Seisenberger, M.U. Ried, T. Endreß, H. Buning, M. Hallek, C. Brauchle, Science 294 (2001) 1929.
[33] B.N.G. Giepmans, S.R. Adams, M.H. Ellisman, R.Y. Tsien, Science 312 (2006) 217.
[34] P. Schwille, Cell Biochem. Biophys. 34 (2001) 383.
[35] J. Enderlein, I. Gregor, D. Patra, J. Fitter, Curr. Pharm. Biotechnol. 5 (2004) 155.
[36] S. Felekyan, R. Kühnemuth, V. Kudryavtsev, C. Sandhagen, W. Becker, C.A.M. Seidel, Rev. Sci. Instrum. 76 (2005) 083104.
[37] C. Eggeling, J. Widengren, L. Brand, J. Schaffer, S. Felekyan, C.A.M. Seidel, J. Phys. Chem. A 110 (2006) 2979.
[38] S. Ruttinger, R. Macdonald, B. Kramer, F. Koberling, M. Roos, E. Hildt, J. Biomed. Opt. 11 (2006) 024012.
[39] S.W. Hell, Nat. Biotechnol. 21 (2003) 1347.
[40] K.I. Willig, S.O. Rizzoli, V. Westphal, R. Jahn, S.W. Hell, Nature 440 (2006) 935.
[41] R.A.L. Vallee, M. Cotlet, M. Van der Auweraer, J. Hofkens, K. Mullen, F.C. De Schryver, J. Am. Chem. Soc. 126 (2004) 2296.

[42] R.A.L. Vallee, P. Marsal, E. Braeken, S. Habuchi, F.C. De Schryver, M. Van der Auweraer, D. Beljonne, J. Hofkens, J. Am. Chem. Soc. 127 (2005) 12011.
[43] R.A.L. Vallee, N. Tomczak, L. Kuipers, G.J. Vancso, N.F. van Hulst, Phys. Rev. Lett. 91 (2003) 038301.
[44] M.D. Mason, K. Ray, R.D. Grober, G. Pohlers, J. Cameron, Phys. Rev. Lett. 93 (2004) 073004.
[45] J.C. Scaiano, H. Garcia, Acc. Chem. Res. 32 (1999) 783.
[46] G. Calzaferri, S. Huber, H. Maas, C. Minkowski, Angew. Chem. Int. Ed. 42 (2003) 3732.
[47] D. Bruhwiler, G. Calzaferri, Micropor. Mesopor. Mater. 72 (2004) 1.
[48] S. Hashimoto, J. Kiuchi, J. Phys. Chem. B 107 (2003) 9763.
[49] S. Hashimoto, S. Yamashita, Chem. Phys. Chem. 5 (2004) 1585.
[50] S. Hashimoto, K. Uehara, K. Sogawa, M. Takada, H. Fukumura, Phys. Chem. Chem. Phys. 8 (2006) 1451.
[51] C. Seebacher, J. Rau, F.W. Deeg, C. Bräuchle, S. Altmaier, R. Jäger, P. Behrens, Adv. Mater. 13 (2001) 1374.
[52] M. Pfenniger, G. Calzaferri, Chem. Phys. Chem. 1 (2000) 211.
[53] C. Seebacher, C. Hellriegel, F.W. Deeg, C. Bräuchle, S. Altmaier, P. Behrens, K. Müllen, J. Phys. Chem. B 106 (2002) 5591.
[54] C. Hellriegel, J. Kirstein, C. Brauchle, V. Latour, T. Pigot, R. Olivier, S. Lacombe, R. Brown, V. Guieu, C. Payrastre, A. Izquierdo, P. Mocho, J. Phys. Chem. B 108 (2004) 14699.
[55] C. Hellriegel, J. Kirstein, C. Brauchle, New J. Phys. 7 (2005) 23.
[56] Y. Fu, F.M. Ye, W.G. Sanders, M.M. Collinson, D.A. Higgins, J. Phys. Chem. B 110 (2006) 9164.
[57] C. Seebacher, C. Hellriegel, C. Bräuchle, M. Ganschow, D. Wöhrle, J. Phys. Chem. B 107 (2003) 5445.
[58] B.F. Sels, D.E. De Vos, P.A. Jacobs, Catal. Rev. 43 (2001) 443.
[59] L. Latterini, F. Elisei, G.G. Aloisi, U. Costantino, M. Nocchetti, Phys. Chem. Chem. Phys. 4 (2002) 2792.
[60] M.B.J. Roeffaers, B.F. Sels, D. Loos, C. Kohl, K. Müllen, P.A. Jacobs, J. Hofkens, D.E. De Vos, Chem. Phys. Chem. 6 (2005) 2295.
[61] M.B.J. Roeffaers, B.F. Sels, H. Uji-i, F.C. De Schryver, P.A. Jacobs, D.E. De Vos, J. Hofkens, Nature 439 (2006) 572.
[62] M. Boudart, A. Aldag, J.E. Benson, N.A. Dougharty, C.G. Harkins, J. Catal. 6 (1966) 92.
[63] M.B.J. Roeffaers, B.F. Sels, H. Uji-i, B. Blanpain, P. L'hoëst, P.A. Jacobs, F.C. De Schryver, J. Hofkens, D.E. De Vos, Angew. Chem. Int. Ed. 10 (2007) 1706–1709.
[64] M. Choura, N.M. Belgacem, A. Gandini, Macromolecules 29 (1996) 3839.
[65] H. Garcia, S. Garcia, J. Perez-Prieto, J.C. Scaiano, J. Phys. Chem. 100 (1996) 18158.
[66] M.B.J. Roeffaers, G. De Cremer, H. Uji-i, B. Muls, B.F. Sels, P.A. Jacobs, F.C. De Schryver, D.E. De Vos, J. Hofkens, Proc. Natl. Acad. Sc. U.S.A., submitted for publication.